ARTICLE

Ultrasensitive, Multiplexed Detection of Cancer Biomarkers Directly in Serum by Using a Quantum Dot-Based Microfluidic Protein Chip

Mei Hu,[†] Juan Yan,[‡] Yao He,[‡,∥] Haoting Lu,[†] Lixing Weng,[§] Shiping Song,[‡] Chunhai Fan,[*,‡] and Lianhui Wang[*,†]

[†]Laboratory of Advanced Materials, Fudan University, 220 Handan Road, Shanghai 200433, People's Republic of China, [‡]Laboratory of Physical Biology, Shanghai Institute of Applied Physics, Chinese Academy of Sciences, Shanghai 201800, People's Republic of China, [§]School of Life Sciences, Fudan University, Shanghai 200433, People's Republic of China, and [∥]Functional Nano and Soft Materials Laboratory, Suzhou University, Jiangsu 215123, People's Republic of China

ABSTRACT Sensitive and selective detection for cancer biomarkers are critical in cancer clinical diagnostics. Here we developed a microfluidic protein chip for an ultrasensitive and multiplexed assay of cancer biomarkers. Aqueous-phase-synthesized CdTe/CdS quantum dots (aqQDs) were employed as fluorescent signal amplifiers to improve the detection sensitivity. Secondary antibodies (goat anti-mouse IgG) were conjugated to luminescent CdTe/CdS QDs to realize a versatile fluorescent probe that could be used for multiplexed detection in both sandwich and reverse phase immunoassays. We found that our microfluidic protein chip not only possessed ultrahigh femtomolar sensitivity for cancer biomarkers, but was selective enough to be directly used in serum. This protein chip thus combines the high-throughput capabilities of a microfluidic network with the high sensitivity and multicolor imaging ability offered by highly fluorescent QDs, which can become a promising diagnostic tool in clinical applications.

KEYWORDS: quantum dots · microfluidic network · protein chip · cancer biomarkers detection · multiplex target detection

*Address correspondence to fchh@sinap.ac.cn, wlhui@fudan.edu.cn.

Received for review October 13, 2009 and accepted December 21, 2009.

Published online December 30, 2009. 10.1021/nn901404h

Semiconductor quantum dots (QDs) have attracted intensive attention during the last two decades. Particularly, the QDs are regarded as promising fluorescent probes due to their unique properties (*e.g.*, size-tunable emission, broad absorption, narrow and symmetric photoluminescence spectra, strong luminescence, and robust photostability).[1−7] The QDs, which are synthesized in organic phase, often possess a high photoluminescent quantum yield (PLQY ~60−85%) and narrow size distribution. They, nevertheless, require additional post-treatment (*e.g.*, stabilizer exchange, silica/polymer coating) to impart their water dispersibility for biological applications.[3,6,8−10] In contrast, the QDs that are directly prepared in the aqueous phase (aqQDs) possess excellent aqueous dispersibility because their stabilizers (*e.g.*, thiols) are naturally water-dispersible.[11] Recently, highly luminescent aqQDs have been readily achieved through several strategies (*e.g.*, hydrothermal method, microwave irradiation (MWI)-based strategy).[12,13] Particularly, the CdTe aqQDs[14,15] and core−shell aqQDs[16] with PLQY of 60−80%, were successfully prepared in our recent studies. However, widespread biological applications (*e.g.*, bioimaging and biodetection) of aqQDs are still hampered by the difficulty in developing a robust and versatile method for conjugating aqQDs with biomolecules (*e.g.*, proteins,[5,6,17−19] peptides,[20,21] and DNA[22,23]). We herein report the synthesis of antibody-conjugated aqQDs with strong photoluminescence and robust stability and an aqQD-based microfluidic protein chip for ultrahigh sensitive, selective, and multiplex detection of cancer biomarkers.

The QD-based bioconjugates were already applied into ELISA,[24,25] Western blotting,[26] and microarray[27] for protein assays.[28] However, all of these techniques are based on a static solid/liquid interface reaction. In such systems, QDs are less active than a small molecular dye because of steric hindrance and are prone to deposit on surfaces. To address this challenge, microfluidic chips based on the manipulation of a continuous liquid flow through microfabricated channels are introduced into our work (Figure 1a). Microfluidic chips do not require expensive automated spotting robots and strict reaction conditions such as humidity and temperature.[29,30] They have the ability to screen for and detect multiple samples with minimal sample processing and handling.[31] Microfluidic biochips are

promising platforms to achieve rapid, sensitive, and high-throughput bioassay of DNA,[32−34] proteins,[33,35−37] bacteria,[38,39] and virals.[40,41] More important, the ambulatory fluid accelerates the reaction between QD probes and targets, and prevents QDs from nonspecific deposition at surfaces. From this point of view, microfluidic biochips are better platforms to exhibit the advantages of QDs. We have previously demonstrated that aqQDs can be integrated within the microfluidic system, leading to high-sensitivity protein detection.[42] In this study, we designed a versatile fluorescent probe by conjugating secondary antibodies (goat anti-mouse IgG), aqQDs, and found that the aqQD-based protein chip could rapidly detect carcinoma embryonic antigen (CEA) and α-fetoprotein (AFP) with high sensitivity and selectivity, even in human serum and in the format of both sandwich immunoassay and reverse phase immunoassay (Figure 1b). Multicolor imaging and multiplexed bioassay using QDs with different emission wavelengths were also developed.

RESULTS AND DISCUSSION

QDs conjugated with antibodies (Abs) are often employed for biological labeling and staining.[43] We coupled aqQDs with secondary Abs (goat anti-mouse IgG) as a versatile probe that could recognize any primary Abs from a mouse. Covalent QD conjugation is most commonly based on cross-linking reactions between amine and carboxylic acid groups, between amine and sulfhydryl groups, or between aldehyde and hydrazide functions. An advantage of the amine−carboxylic acid cross-linking method is that most proteins contain primary amine and carboxylic acid groups and do not need chemical modifications before QD conjugation.[43] However, this technique may bring about instability of the QD when chemically modifying its stabilizer cap and the cross-reaction of the QD-COOH groups with multiple amines on biomolecules.[44] To overcome this problem, we studied the key factors influencing the chemical stability of QDs and demonstrated an elaborate aqQD-based bioconjugating strategy.

Sodium dodecyl sulfate polyacrylamide gel electrophoresis (SDS-PAGE) was performed to confirm QD-IgG conjugates, determining relative sizes and molecular weights of QD conjugates. The mobility of the proteins in SDS-PAGE is determined by the mass/charge ratio of denatured protein chains carrying SDS, which imparts negative charge to them.[25] After running gels loaded with QDs (lane 1 in Figure S1), QD-IgG conjugates (lanes 2−7 in Figure S1), and goat anti-mouse IgG (lane 8 in Figure S1), differences of relative molecular weights were apparent. In lane 1 (QDs) of panel a, we could observe one fluorescent band at 15 kD under UV illumination. In lane 8 (IgG) of panel b, after the gel was stained by Coommassie Blue, there was a prominent band at 150 kD and several bands at upper positions, which indicated that there are dimers and polymers in the commercial goat anti-mouse IgG, whose monomer molecular weight should be 150 kD. After conjugation with IgG, the fluorescent band of the QDs shifted from 15 to 150 kD and upper positions. After stained by Coomassie blue, we could observe that the bands of QD-IgG conjugates coincided with the bands

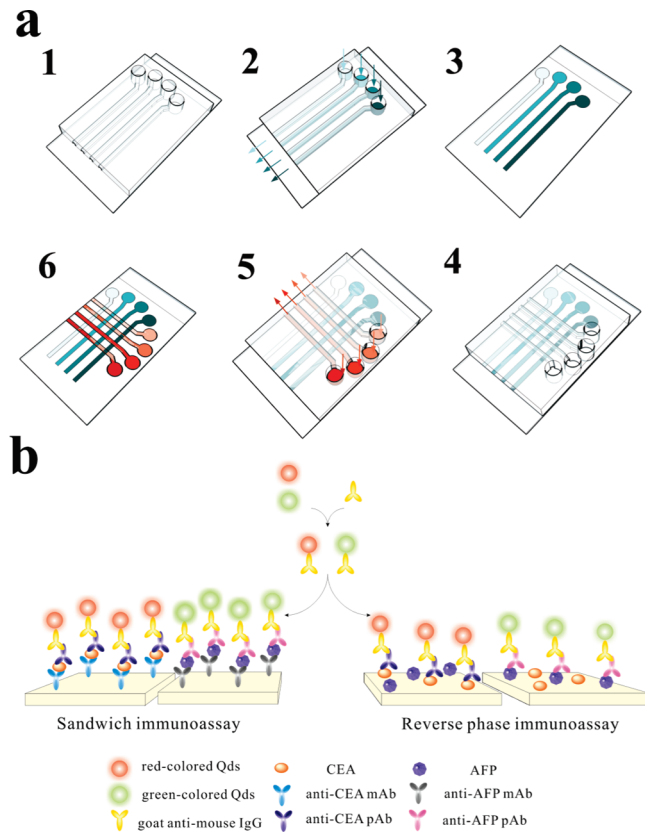

Figure 1. (a) Schematic illustration of the microchannel network. (1) First, a PDMS piece was placed in a silyated slide; (2) The solutions were flowed through the channels, and the first layer of protein was immobilized; (3) The first PDMS piece was removed; (4) The other PDMS piece was placed on the substrate with channels perpendicular to the first PDMS piece; (5) Other solutions were flowed; (6) A two-dimensional array was formed above the chip. (b) Schematic illustration of a sandwich immunoassay and reverse phase immunoassay based on QD-IgG fluorescent probes and microfluidic protein chip.

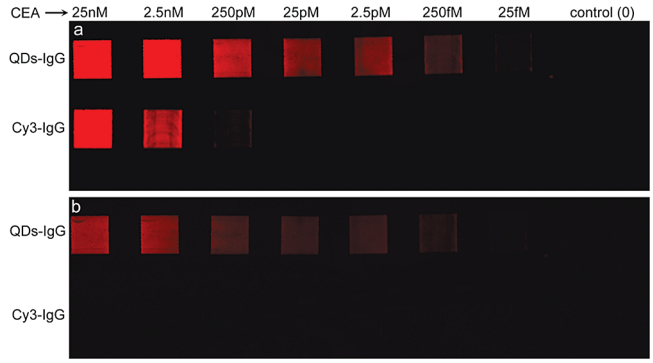

Figure 2. Comparison of the brightness of QD-IgG and Cy3-IgG as signal probes: (a) illuminated by UV (365 nm) and (b) illuminated by green light (546 nm). The fluorescent images of the microchannel network arrays were captured using QD-IgG and Cy3-IgG with the target proteins (CEA) concentration rang from 25 nM to 25 fM.

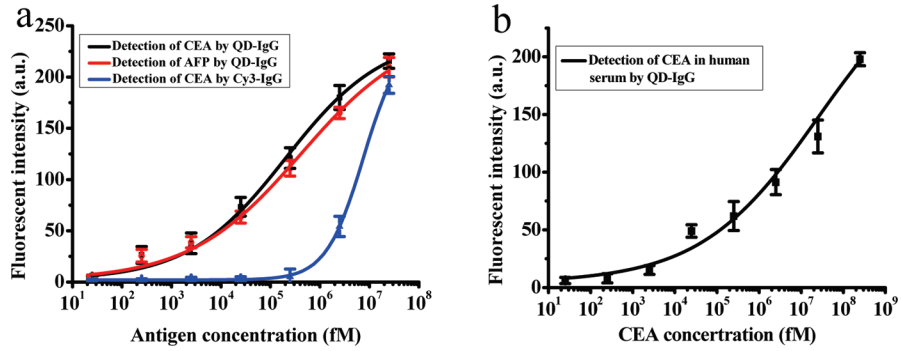

Figure 3. (a) Dose−response calibration curves for CEA and AFP based on the QD-IgG and microfluidic protein chip. CEA was also detected by Cy3-IgG as a comparison. The fluorescent images of parallel detection of CEA and AFP samples (concentrations of CEA and AFP ranged from 25 fM to 25 nM) in five parallel microchannels were captured (Figure S4). The standard curves were fitted by a logistic model. (b) The dose−response calibration curve for CEA in human serum based on the QD-IgG probes and microfluidic network chip. The fluorescent images of parallel detection of CEA samples (concentrations of CEA ranged from 25 fM to 250 nM) in five parallel microfluidic channels were captured (figure not shown). The standard curve was fitted by a logistic model.

of free IgG. The increase of mass due to the addition of QDs to IgG is compensated by the increase of the overall charge density of the conjugate. These results validated the successful covalent conjugation of QDs and IgG.

SDS-PAGE was also used to test different conjugation conditions. Through comparison of QD-IgG conjugates' fluorescent intensity in electrophoresis bands under different conjugation conditions, we could deduce the optimal conjugation condition. Among the various influence factors, the molar ratio between QDs and cross-linkers was most critical. To ensure sufficient reaction of IgG with QDs, excessive QDs were added. The molar ratio between QDs and IgG was maintained to be 2:1. Then we changed the molar ratio between QDs, *N*-(3-dimethylaminopropyl)-*N*-ethylcarbodiimde hydrochloride (EDC), and *N*-hydroxysuccinimide (NHS). The molar ratio between QDs and EDC was first examined (Figure S1). The fluorescent intensity of the conjugate band was enhanced along with the accretion of the molar ratio of EDC (lanes 2−7 in Figure S1). When the molar ratio between QDs and EDC reached 1:800 (lane 6 in Figure S1), the bands of the conjugates were the brightest. But under the molar ratio of 1:1200, slight precipitation was observed after the QD-IgG conjugate was stored at 4 °C overnight. Based on such results, we maintained the molar ratio (QDs/EDC) at 1:800.

In addition, we tested combining EDC and NHS as cross-linking reagents and examined the conjugates with SDS-PAGE (Figure S2). EDC reacts with a carboxyl to form an amine-reactive *O*-acylisourea intermediate. However, the intermediate is also susceptible to hydrolysis, making it unstable and short-lived in aqueous solution. The addition of NHS stabilizes the amine-reactive intermediate by converting it to an amine-reactive NHS ester, thus, increasing the efficiency of EDC-mediated coupling reactions.[45,46] The amine-reactive NHS ester intermediate has sufficient stability to permit two-step cross-linking procedures, which allow the carboxyl groups on protein to remain unaltered and avoid cross-linking of IgG. As expected, efficiency of EDC-mediated coupling is increased in the presence of NHS. When the ratio of QDs, EDC, and NHS reach 1:800:1600, efficiency of conjugation as well as the stability of conjugates was best. Under this optimal conjugation condition, there was a slight decrease in PLQY (less than 20%) and stability of QDs (Figure S3). The QD-IgG conjugates were highly stable and could be stored for at least 3 months without apparent aggregation.

The as-prepared QD-IgG was used as a versatile fluorescent probe for the detection of cancer biomarkers (*e.g.*, CEA and AFP) in the microfluidic protein chip. Given that QDs exhibit significantly higher PLQY and photostability than organic dyes, we expect that the integration of QDs in microfluidic protein chips, could significantly improve the detection sensitivity. Figure 2 compared the signal brightness of protein chip using Cy3-IgG and red-colored emitting QD-IgG as probes, respectively. In both systems, the protein chip was challenged with target proteins (CEA) in the concentration range from 25 fM to 25 nM, covering 6 orders of magnitude. Indeed, QD probes showed high brightness and a concentration-dependent intensity gradient, leading to a limit of detection (LOD) of 250 fM and a broad dynamic range of 5 orders of magnitude; while signal of Cy3 probes was only visible at higher target concentration (>250 pM). More significantly, the signal of Cy3 could be visualized only under its optimum excitation wavelength (~546 nm), while the fluorescent signal of QDs could be detected under both green light (546 nm) and UV light (365 nm) illumination. This is due to the characteristic broad absorption of QDs, that is, QDs can be excited by any wavelength from UV to red light, whereas organic dyes are restricted by their narrow excitation spectra,[5] which significantly reduces the cost

for additional excitation sources in multiplexed detection.

Large background and high false-positive rate are serious problems for most protein chips.[24,47,48] We then adopted a combination of methods to reduce the background. The QD-IgG conjugate was blocked with bovine serum albumin (BSA, 5%), and Tween-20 was added into the washing buffer to minimize nonspecific adsorption. Moreover, the fluorescent signal of QDs was stabilized with the use of reduced L-glutathione, which possibly avoided oxidation of QDs in air.[26,42] We found that such steps significantly enhanced the signal-to-noise ratio (S/B). In control experiments without such steps, the background was so significant that it was almost comparable to the target concentration of 2.5 nM.

In principle, the versatile fluorescent probe prepared in this experiment could be applied to detect all targets with appropriate concentrations since the goat anti-mouse IgG conjugated with the QDs could react with any Abs originated from mouse. As a proof-of-concept, CEA and AFP were used as model targets in our study. Figure 3a demonstrated a typical dose−response result for CEA and AFP at a wide concentration ranging from 25 fM to 25 nM. The LOD is estimated to be 250 fM for both CEA and AFP (S/N>3). The entire statistic is based on five independent experiments to make sure the reliability of this assay. As a comparison, the LOD for CEA using Cy3-IgG as probes is 2.5 nM in the same chip, which is 4 orders of magnitude higher than that for QD-IgG. Therefore, the detection system using QD-IgG as a fluorescent probe provided ultrahigh sensitivity could exert more potential in early phase detection of cancers.

It is critically important to evaluate the performance of our microfluidic protein chip in complicated samples (*e.g.*, sera) for real-world applications. We then tried to detect CEA in human serum, with a concentration ranged of 25 fM∼250 nM. Figure 3b displayed a typical dose−response result for CEA. The LOD was estimated to be 2.5 pM, 10-fold higher as compared with the detection in PBS buffer. The possibility is that a large amount of serum albumin present in the serum disturbed the immunoreaction between antigens (Ags) and Abs to a certain degree, and they might block unoccupied sites of the chip. Despite that, the sensitivity is still comparable to the commercial CEA ELISA KIT (*e.g.*, the LODs for CEA and AFP in ELISA KITs (Lico-Bio, Shanghai) were 5 pM and 7 pM, respectively). Of note, our data were collected with a fluorescent microscope, while higher sensitivity could be achieved *via* the use of better equipment (*e.g.*, our preliminary study using a laser-illuminated fluorescent scanner showed improved sensitivity of at least an order of magnitude).

Due to the contribution of broad absorption with narrow photoluminescence spectra of QDs, the multicolored QDs with the different sizes could be illuminated synchronously by a single excitation wavelength. In contrast, organic dyes with the different maximal

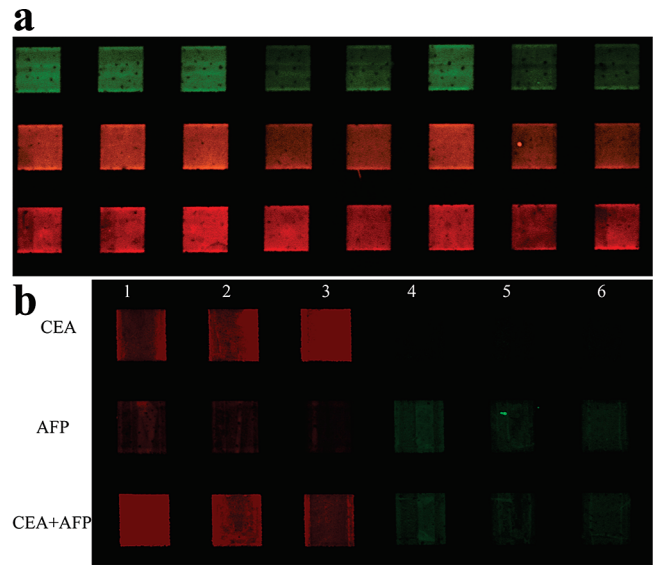

Figure 4. (a) Multicolored imaging by green-, orange-, and red-colored QD-IgG probes based on microfluidic protein chip. (b) Multiplexed labeling for CEA and AFP by red and green-colored emitting QD-IgG probes based on reverse phase immunoassay and microfluidic protein chip. First, CEA, AFP, and the mixture solution of CEA and AFP were immobilization on the silyated slide along the horizontal microchannels side by side. The concentration of each antigen was 25 pM. Then the mixture solution of anti-CEA Abs and anti-AFP Abs was flowed along the perpendicular microchannels. After that, the microchannels 1−3 were filled with red-colored QD-IgG and the microchannels 4−6 were filled with green-colored emitting QD-IgG.

emission wavelengths must be illuminated by the different optimal excitation wavelengths. For example, the optimal excitation wavelengths of FITC and Cy3 are 495 and 552 nm, respectively. For imaging of both FITC and Cy3, we must change the optical filters within the microscope. To demonstrate this advantage of QDs, the proof-of-concept experiment was explored. Three types of QDs with different emission wavelengths were employed in the same chip for detection of CEA simultaneously (the concentration of CEA is 25 pM). Under the UV illumination, as shown in Figure 4a, fluorescent signals with three colors were observed. This advantage is clearly useful in multiplexed detection.

The sandwich immunoassay is usually employed to quantitatively detect targets, while the reverse phase immunoassay is prevalent for qualitative assay of protein−protein interactions in proteome studies. As a versatile fluorescent probe, QD-IgG also has the potential in this field. We used mixture solution of CEA and AFP as the model (Figure 4b). In this experiment, CEA, AFP, and the mixture solution of CEA and AFP were immobilized on the silyated slide along the horizontal microchannels side by side. Then the mixture solution of anti-CEA Abs and anti-AFP Abs was flowed through the perpendicular microchannels. After that, the perpendicular microchannels 1−3 were filled with red-color emitting QD-IgG and the perpendicular microchannels 4−6 were filled with green-color emitting QD-IgG. Based on the immunoreaction between Ags and Abs, CEA could bind to anti-CEA Abs while AFP to anti-AFP

Abs. As a result, the mixture solution of CEA and AFP could be distinguished by anti-CEA Abs as well as anti-AFP Abs *via* red and green colors detected in the horizontal channels. As shown in Figure 4b, while minimal cross-talk was observed, we could reliably identify positive signals for both CEA and AFP *via* their individual colors, which implies the applicability of this approach to proteomic studies.

CONCLUSIONS

In summary, the present study has successfully conjugated QDs with a secondary antibody. This bionanohybrid exhibits excellent performance as a fluorescent probe in protein assays. The QD-IgG conjugate, combined with a microfluidic protein chip, improved the detection limits of cancer biomarkers up to 250 fM, which represents a sensitivity improvement up to 4 orders of magnitude as compared to organic dyes (*e.g.*, commercially available Cy3-Abs conjugates). Besides, multicolored imaging was realized and potentially useful for multiplexed detection in proteomic studies. This study thus opens a new path for practical clinical and proteomic applications of protein chips.

METHODS

Materials and Reagents. Silylated slides (aldehyde activated) were obtained from CEL Associates (Pearland, U.S.A.). Sylgard184 was purchased from Dow Corning Co. Ltd. (Shanghai, China). All antigens (target proteins, Ags) were purchased from Industries International (Concord, U.S.A.). Monoclonal antibodies (mAbs) and polyclonal antibodies (pAbs) were purchased from USBIO. Goat anti-mouse IgG-Cy3, bovine serum albumin (BSA), *N*-(3-dimethylaminopropyl)-*N*-ethylcarbodiimde hydrochloride (EDC), *N*-hydroxysuccinimide (NHS), and other chemical reagents were purchased from Sigma-Aldrich (St. Louis, MO). Tween-20 was purchased from Fluka. Silicon patterns were fabricated by Shanghai Institute of Microsystem and Information Technology (SIMIT), Chinese Academy of Sciences. Syringe pump was purchased from Zhejiang University (Hangzhou, China).

Nearly monodispersed CdTe/CdS core−shell QDs capped with mercaptopropionic acid (MPA) were obtained *via* microwave irradiation as described in our previous work.[49] Three types of QDs with different sizes were used. The maximum emission wavelengths were 530 (green), 564 (orange), and 595 nm (red), respectively. These QDs are very stable in PBS buffer (150 mM, pH 7.3) at 4 °C. No significant changes in the photoluminescence were detected during several months.

Preparation of QD-IgG Conjugates. Carbodiimine chemistry was applied for conjugation using EDC and NHS as zero-length cross-linkers.[25,43] Carboxylic acid groups of MPA displayed on the QDs surface bound with the amine groups of proteins.

We tested different reaction conditions, including reaction time, concentrations, and cross-linkers. The following is the optimal protocol developed in the course of this study. First, water-dispersed QDs (in 150 mM PBS, pH 7.3) were activated with EDC/NHS. To 60 μL of QDs (12 μM), add 17.25 μL of EDC (33.4 mM in H_2O) and 16.25 μL of NHS (70.9 mM in H_2O). The reaction solution was incubated at 25 °C for 15 min with gentle shaking. EDC is easily hydrolytic and should be dissolved in water immediately before use. Then 27 μL of goat anti-mouse IgG (13.3 μM) in PBS buffer was added to the activated QDs. The molar ratio of QD/EDC/NHS/IgG was calculated as 1:800:1600:0.5.

The mixture was incubated at 25 °C for 2 h under shaking in a dark and then kept overnight at 4 °C. No obvious precipitation occurred after this conjugation reaction. Both the free nonconjugated QDs and byproduct isourea were removed by ultrafiltration using 100 K Nanosep centrifugal devices by centrifugation at 5000 rmp for 15 min. The lower phase, containing free QDs and isourea, were discarded. To wash the conjugate and reduce the impurities, the upper phase, containing QD-IgG, was diluted by 300 μL PBS buffer, and additionally subjected to centrifugation at 5000 rmp for 15 min. This washing step was repeated twice. The conjugate was recovered by 100 μL of PBS and transferred to a new Eppendorf tube and then stored at 4 °C in a dark until use.

Characterization of QD-IgG Conjugates by Sodium Dodecyl Sulfate Polyacrylamide Gel Electrophoresis (SDS-PAGE). The formation of IgG-conjugated QDs was confirmed by SDS-PAGE. Different conjugated conditions, mainly the mole ratio between QDs, EDC, NHS and IgG were also examined by SDS-PAGE. A total of 8% resolving gel and 4% stocking gel were used. Acrylamide/bisacrylamide monomer, DI water, gel buffer, and SDS were mixed with fresh ammonium persulfate and TEMED for the resolving gel, loaded into sealed gel caster, overlaid with DI water to exclude oxygen and allowed to polymerize. After polymerization, the DI water was decanted and the stacking gel was made and layered on top of the polymerized resolving gel. Plastic 10-well combs were inserted into the stacking gel and polymerization allowed to occur (~30 min). The combs were then removed, gels assembled into electrophoresis units. Then wells were thoroughly washed with water to remove acrylamide and excess radicals. Samples were diluted in sample buffer (62.5 mM Tris, 2% SDS, 10% glycerol, 0.2% BMB) for 15 min, loaded into the gels, and run for 90 min at 120 V. Tank buffer was 250 mM Gly, 192 mM Tris with 0.1% SDS (pH8.3). Finally, the gel was stained for protein with Coomassie brilliant blue.

Fabrication of Microfluidic Channels. Master molds for the microchannels were fabricated using standard photolithographic methods with SU-8 epoxy based negative resists. A 10:1 v/v mixture of polydimethylsiloxane (PDMS) prepolymer and curing agent was prepared, degassed, and poured on the patterned glass flat. The PDMS was cured at 90 °C for 2 h, removed from the substrate, and baked overnight at 90 °C to fully cure the chip. Inlet and outlet holes were drilled in the PDMS using a sharpened needle. PDMS layers containing 22 microchannels. Diameter of the microchannels: width = 150 μm; gap between the channels = 150 μm; height = 30 μm.

Detection of Cancer Biomarkers Using Microfluidic Protein Chip. The PDMS piece was sealed against the silyated slides to form enclosed channels (Figure 1a). Conformal contact is achieved spontaneously through van der Waals interactions between the materials. After the channels were formed, solutions were pulled through the microfluidic channels using a syringe pump. After incubated at 30 °C overnight, the microchannels were rinsed with washing buffer (PBS, containing 0.1% Tween-20) and then removed the first PDMS piece. Then the unoccupied sites were blocking with blocking buffer (150 mM PBS, pH 7.4, 5% BSA) for 1 h. After the immobilization of the first layer, the other PDMS piece, with the direction of its channels perpendicular to the earlier case, was then placed over the patterned area. Other solutions were then flowed through the channels, creating a two-dimensional array of interaction spots. After incubation at 37 °C for 1 h and repeated the rinsing step, the third and fourth layers were immobilized in the same way. Removing the second PDMS piece, chips were imaged with a fluorescent microscope (AxioSkop, ZEISS) equipped with optical filters and a charge-coupled camera (AxioCam MRC5, ZEISS).

In sandwich immunoassay, mAbs (3 μM) were first patterned as capture probes. Then targets and pAbs (3 μM) were immobilized orderly in the perpendicular microchannels. At last, QD-IgG (1 μM) and Cy3-IgG (1 μM) were spotted as fluorescent probes. In reverse phase immunoassay, samples were first immobilized, and then mAbs (3 μM) and QD-IgG (1 μM) were placed.

Acknowledgment. This work was financially supported by the National Natural Science Foundation of China (30425020,

90813010, 20725516, 60537030, 90913014), Ministry of Health (2009ZX10004-301), Ministry of Science and Technology (2006CB933000, 2007CB936000), Shanghai Leading Academic Discipline Project (B113), and Shanghai Government (08PJ14011, 0952 nm04600).

Supporting Information Available: Characterization of QD-IgG conjugates by SDS-PAGE and the fluorescent images of parallel detection of CEA and AFP samples. This material is available free of charge *via* the Internet at http://pubs.acs.org.

REFERENCES AND NOTES

1. Carion, O.; Mahler, B.; Pons, T.; Dubertret, B. Synthesis, Encapsulation, Purification and Coupling of Single Quantum Dots in Phospholipid Micelles for Their Use in Cellular and In Vivo Imaging. *Nat. Protoc.* **2007**, *2*, 2383–2390.
2. So, M. K.; Xu, C. J.; Loening, A. M.; Gambhir, S. S.; Rao, J. H. Self-Illuminating Quantum Dot Conjugates for In Vivo Imaging. *Nat. Biotechnol.* **2006**, *24*, 339–343.
3. Gao, X. H.; Cui, Y. Y.; Levenson, R. M.; Chung, L. W. K.; Nie, S. M. In Vivo Cancer Targeting and Imaging with Semiconductor Quantum Dots. *Nat. Biotechnol.* **2004**, *22*, 969–976.
4. Wu, X. Y.; Liu, H. J.; Liu, J. Q.; Haley, K. N.; Treadway, J. A.; Larson, J. P.; Ge, N. F.; Peale, F.; Bruchez, M. P. Immunofluorescent Labeling of Cancer Marker Her2 and Other Cellular Targets with Semiconductor Quantum Dots. *Nat. Biotechnol.* **2003**, *21*, 452.
5. Jaiswal, J. K.; Mattoussi, H.; Mauro, J. M.; Simon, S. M. Long-Term Multiple Color Imaging of Live Cells Using Quantum Dot Bioconjugates. *Nat. Biotechnol.* **2003**, *21*, 47–51.
6. Bruchez, M.; Moronne, M.; Gin, P.; Weiss, S.; Alivisatos, A. P. Semiconductor Nanocrystals as Fluorescent Biological Labels. *Science* **1998**, *281*, 2013–2016.
7. Liu, W.; Howarth, M.; Greytak, A. B.; Zheng, Y.; Nocera, D. G.; Ting, A. Y.; Bawendi, M. G. Compact Biocompatible Quantum Dots Functionalized for Cellular Imaging. *J. Am. Chem. Soc.* **2008**, *130*, 1274–84.
8. Gopalakrishnan, G.; Danelon, C.; Izewska, P.; Prummer, M.; Bolinger, P. Y.; Geissbuhler, I.; Demurtas, D.; Dubochet, J.; Vogel, H. Multifunctional Lipid/Quantum Dot Hybrid Nanocontainers for Controlled Targeting of Live Cells. *Angew. Chem., Int. Ed.* **2006**, *45*, 5478–5483.
9. Dubertret, B.; Skourides, P.; Norris, D. J.; Noireaux, V.; Brivanlou, A. H.; Libchaber, A. In Vivo Imaging of Quantum Dots Encapsulated in Phospholipid Micelles. *Science* **2002**, *298*, 1759–1762.
10. Kairdolf, B. A.; Mancini, M. C.; Smith, A. M.; Nie, S. Minimizing Nonspecific Cellular Binding of Quantum Dots with Hydroxyl-Derivatized Surface Coatings. *Anal. Chem.* **2008**, *80*, 3029–34.
11. Gaponik, N.; Talapin, D. V.; Rogach, A. L.; Hoppe, K.; Shevchenko, E. V.; Kornowski, A.; Eychmuller, A.; Weller, H. Thiol-Capping of Cdte Nanocrystals: An Alternative to Organometallic Synthetic Routes. *J. Phys. Chem. B* **2002**, *106*, 7177–7185.
12. Zhang, H.; Cui, Z. C.; Wang, Y.; Zhang, K.; Ji, X. L.; Lu, C. L.; Yang, B.; Gao, M. Y. From Water-Soluble Cdte Nanocrystals to Fluorescent Nanocrystal-Polymer Transparent Composites Using Polymerizable Surfactants. *Adv. Mater.* **2003**, *15*, 777–780.
13. Li, L.; Qian, H. F.; Ren, J. C. Rapid Synthesis of Highly Luminescent Cdte Nanocrystals in the Aqueous Phase by Microwave Irradiation with Controllable Temperature. *Chem. Commun.* **2005**, 528–530.
14. He, Y.; Lu, H. T.; Sai, L. M.; Lai, W. Y.; Fan, Q. L.; Wang, L. H.; Huang, W. Synthesis of Cdte Nanocrystals through Program Process of Microwave Irradiation. *J. Phys. Chem. B* **2006**, *110*, 13352–13356.
15. He, Y.; Sai, L. M.; Lu, H. T.; Hu, M.; Lai, W. Y.; Fan, Q. L.; Wang, L. H.; Huang, W. Microwave-Assisted Synthesis of Water-Dispersed Cdte Nanocrystals with High Luminescent Efficiency and Narrow Size Distribution. *Chem. Mater.* **2007**, *19*, 359–365.
16. He, Y.; Lu, H.; Sai, L.; Su, Y.; Hu, M.; Fan, C.; Huang, W.; Wang, L. Microwave Synthesis of Water-dispersed CdTe/CdS/ZnS Core-shell-shell Quantum Dots with Excellent Photostability and Biocompatibility. *Adv. Mater.* **2008**, *20*, 3416–3421.
17. Chan, W. C. W.; Nie, S. M. Quantum Dot Bioconjugates for Ultrasensitive Nonisotopic Detection. *Science* **1998**, *281*, 2016–2018.
18. Chakraborty, S. K.; Fitzpatrick, J. A. J.; Phillippi, J. A.; Andreko, S.; Waggoner, A. S.; Bruchez, M. P.; Ballou, B. Cholera Toxin B Conjugated Quantum Dots for Live Cell Labeling. *Nano Lett.* **2007**, *7*, 2618–2626.
19. Goldman, E. R.; Clapp, A. R.; Anderson, G. P.; Uyeda, H. T.; Mauro, J. M.; Medintz, I. L.; Mattoussi, H. Multiplexed Toxin Analysis Using Four Colors of Quantum Dot Fluororeagents. *Anal. Chem.* **2004**, *76*, 684–688.
20. Cai, W. B.; Chen, X. Y. Preparation of Peptide-Conjugated Quantum Dots for Tumor Vasculature-Targeted Imaging. *Nat. Protoc.* **2008**, *3*, 89–96.
21. Cai, W. B.; Shin, D. W.; Chen, K.; Gheysens, O.; Cao, Q. Z.; Wang, S. X.; Gambhir, S. S.; Chen, X. Y. Peptide-Labeled Near-Infrared Quantum Dots for Imaging Tumor Vasculature in Living Subjects. *Nano Lett.* **2006**, *6*, 669–676.
22. Zhang, C. Y.; Yeh, H. C.; Kuroki, M. T.; Wang, T. H. Single-Quantum-Dot-Based DNA Nanosensor. *Nat. Mater.* **2005**, *4*, 826–831.
23. Tanke, H. J.; Dirks, R. W.; Raap, T. Fish and Immunocytochemistry: Towards Visualising Single Target Molecules in Living Cells. *Curr. Opin. Biotechnol.* **2005**, *16*, 49–54.
24. Woodbury, R. L.; Varnum, S. M.; Zangar, R. C. Elevated Hgf Levels in Sera from Breast Cancer Patients Detected Using a Protein Microarray Elisa. *J. Proteome Res.* **2002**, *1*, 233–7.
25. Wang, S. P.; Mamedova, N.; Kotov, N. A.; Chen, W.; Studer, J. Antigen/Antibody Immunocomplex from Cdte Nanoparticle Bioconjugates. *Nano Lett.* **2002**, *2*, 817–822.
26. Bakalova, R.; Zhelev, Z.; Ohba, H.; Baba, Y. Quantum Dot-Based Western Blot Technology for Ultrasensitive Detection of Tracer Proteins. *J. Am. Chem. Soc.* **2005**, *127*, 9328–9329.
27. Shingyoji, M.; Gerion, D.; Pinkel, D.; Gray, J. W.; Chen, F. Q. Quantum Dots-Based Reverse Phase Protein Microarray. *Talanta* **2005**, *67*, 472–478.
28. Ligler, F. S.; Sapsford, K. E.; Golden, J. P.; Shriver-Lake, L. C.; Taitt, C. R.; Dyer, M. A.; Barone, S.; Myatt, C. J. The Array Biosensor: Portable, Automated Systems. *Anal. Sci.* **2007**, *23*, 5–10.
29. Tadic, S.; Dernick, G.; Juncker, D.; Buurman, G.; Kropshofer, H.; Michel, B.; Fattinger, C.; Delamarche, E. High-Sensitivity Miniaturized Immunoassays for Tumor Necrosis Factor a Using Microfluidic Systems Using Microfluidic Systems. *Lab Chip* **2004**, *4*, 563–569.
30. Golden, J.; Shriver-Lake, L. C.; Sapsford, K. E.; Ligler, F. A "Do-It-Yourself" Array Biosensor. *Methods* **2005**, *37*, 65–72.
31. Delamarche, E.; Juncker, D.; Schmid, H. Microfluidics for Processing Surfaces and Miniaturizing Biological Assays. *Adv. Mater.* **2005**, *17*, 2911–2933.
32. Ueberfeld, J.; McKenna, B.; Rubin-Bejerano, I.; Verstrepen, K.; Ehrlich, D. J. Reaction-Mapped Quantitative Multiplexed Polymerase Chain Reaction on a Microfluidic Device. *Anal. Chem.* **2008**, *80*, 7430–7436.
33. Fernandes, R.; Yi, H. M.; Wu, L. Q.; Rubloff, G. W.; Ghodssi, R.; Bentley, W. E.; Payne, G. F. Thermo-Biolithography: A Technique for Patterning Nucleic Acids and Proteins. *Langmuir* **2004**, *20*, 906–913.
34. Anderson, R. C.; Su, X.; Bogdan, G. J.; Fenton, J. A Miniature Integrated Device for Automated Multistep Genetic Assays. *Nucleic Acids Res.* **2000**, *28*, E60.
35. Ko, Y. J.; Maeng, J. H.; Ahn, Y.; Hwang, S. Y.; Cho, N. G.; Lee, S. H. Microchip-Based Multiplex Electro-Immunosensing System for the Detection of Cancer Biomarkers. *Electrophoresis* **2008**, *29*, 3466–3476.

36. Su, J.; Bringer, M. R.; Ismagilov, R. F.; Mrksich, M. Combining Microfluidic Networks and Peptide Arrays for Multi-Enzyme Assays. *J. Am. Chem. Soc.* **2005**, *127*, 7280–7281.
37. Sanders, G. H. W.; Manz, A. Chip-Based Microsystems for Genomic and Proteomic Analysis. *TrAC, Trends Anal. Chem.* **2000**, *19*, 364–378.
38. Shih, P. H.; Shiu, J. Y.; Lin, P. C.; Lin, C. C.; Veres, T.; Chen, P. On Chip Sorting of Bacterial Cells Using Sugar-Encapsulated Magnetic Nanoparticles. *J. Appl. Phys.* **2008**, 103.
39. Liu, W. T.; Zhu, L. Environmental Microbiology-on-a-Chip and Its Future Impacts. *Trends Biotechnol.* **2005**, *23*, 174–179.
40. Liu, W. T.; Zhu, L.; Qin, Q. W.; Zhang, Q.; Feng, H. H.; Ang, S. Microfluidic Device as a New Platform for Immunofluorescent Detection of Viruses. *Lab Chip* **2005**, *5*, 1327–1330.
41. Lopez, M. M.; Bertolini, E.; Olmos, A.; Caruso, P.; Gorris, M. T.; Llop, P.; Penyalver, R.; Cambra, M. Innovative Tools for Detection of Plant Pathogenic Viruses and Bacteria. *Int. Microbiol.* **2003**, *6*, 233–243.
42. Yan, J.; Hu, M.; Li, D.; He, Y.; Zhao, R.; Jiang, X.; Song, S.; Wang, L.; Fan, C. A Nano- and Micro- Integrated Protein Chip Based on Quantum Dot Probes and a Microfluidic Network. *Nano Res.* **2008**, *1*, 490–496.
43. Xing, Y.; Chaudry, Q.; Shen, C.; Kong, K. Y.; Zhau, H. E.; WChung, L.; Petros, J. A.; O'Regan, R. M.; Yezhelyev, M. V.; Simons, J. W.; Wang, M. D.; Nie, S. Bioconjugated Quantum Dots for Multiplexed and Quantitative Immunohistochemistry. *Nat. Protoc.* **2007**, *2*, 1152–1165.
44. Medintz, I. L.; Uyeda, H. T.; Goldman, E. R.; Mattoussi, H. Quantum Dot Bioconjugates for Imaging, Labelling, and Sensing. *Nat. Mater.* **2005**, *4*, 435–446.
45. DeSilva, N. S. Interactions of Surfactant Protein D with Fatty Acids. *Am. J. Respir. Cell Mol. Biol.* **2003**, 757–770.
46. Grabarek, Z.; Gergely, J. Zero-Length Crosslinking Procedure with the Use of Active Esters. *Anal. Biochem.* **1990**, 131–135.
47. Sia, S. K.; Linder, V.; Parviz, B. A.; Siegel, A.; Whitesides, G. M. An Integrated Approach to a Portable and Low-Cost Immunoassay for Resource-Poor Settings. *Angew. Chem., Int. Ed.* **2004**, *43*, 498–502.
48. Schweitzer, B.; Roberts, S.; Grimwade, B.; Shao, W.; Wang, M.; Fu, Q.; Shu, Q.; Laroche, I.; Zhou, Z.; Tchernev, V. T.; Christiansen, J.; Velleca, M.; Kingsmore, S. F. Multiplexed Protein Profiling on Microarrays by Rolling-Circle Amplification. *Nat. Biotechnol.* **2002**, *20*, 359–65.
49. He, Y.; Lu, H. T.; Sai, L. M.; Lai, W. Y.; Fan, Q. L.; Wang, L. H.; Huang, W. Microwave-Assisted Growth and Characterization of Water-Dispersed Cdte/Cds Core-Shell Nanocrystals with High Photoluminescence. *J. Phys. Chem. B* **2006**, *110*, 13370–13374.